Check for updates

ChemPubSoc Europe

DOI: 10.1002/cplu.201500310

CHEMPLUSCHEM Full Papers

# Selective Liquid-Phase Hydrogenation of a Nitro Group in Substituted Nitrobenzenes over $Au/Al_2O_3$ Catalyst in a Packed-Bed Flow Reactor

Alexey L. Nuzhdin,[a] Boris L. Moroz,[a, b] Galina A. Bukhtiyarova,*[a] Sergey I. Reshetnikov,[a] Pavel A. Pyrjaev,[a] Pavel V. Aleksandrov,[a] and Valerii I. Bukhtiyarov[a, b]

A series of substituted nitrobenzenes with the general formula $XC_6H_4NO_2$ (X = Cl, $CH{=}CH_2$, or $C(O)CH_3$) dissolved in toluene were reduced with hydrogen over the 1.9% $Au/Al_2O_3$ catalyst at 60–110 °C and 10–20 bar in a three-phase packed-bed reactor operating in up-flow mode. Under these conditions, hydrogenation of isomeric $ClC_6H_4NO_2$ gives exclusively chloroanilines. Hydrogenation of 3-$CH_2CHC_6H_4NO_2$ and 4-$CH_3C(O)C_6H_4NO_2$ leads to the formation of 3-$CH_2CHC_6H_4NH_2$ and 4-$CH_3C(O)C_6H_4NH_2$ with selectivities of up to 93 and 97% at substrate conversions of 98 and 100%, respectively. Smooth catalyst deactivation was observed regardless of which substituted nitrobenzene was taken for hydrogenation. According to the results obtained by temperature-programmed oxidation of the spent catalyst, a carbonaceous deposit formed that might block the catalyst surface. Almost complete regeneration of the supported gold catalyst with retention of its high selectivity to hydrogenation of a nitro group was achieved in a flow of air at temperatures up to 400 °C to eliminate carbonaceous deposits.

## Introduction

Functionalized anilines are commercially valuable products that are intermediates in the manufacture of variety of agrochemicals, herbicides, polymers, pharmaceuticals, and dyes.[1,2] Conventional techniques for producing anilines are based on the reduction of a nitro group with stoichiometric amounts of reducing agents, such as iron in acid media (Bechamp process), $H_2S$, or NaHS, but these processes are accompanied by the formation of a large amount of harmful waste products and demonstrate low selectivity when used for the reduction of substituted nitrobenzenes.[2] Catalytic hydrogenation is undoubtedly a more economical and environmentally friendly alternative for the production of functionalized anilines. Many excellent monographs and reviews have described catalysts, reaction media, and conditions required to achieve selective reduction of the nitro group with hydrogen in the presence of other reducible groups (C–Cl, C=O, or C=C bonds).[2,3] The authors unanimous state that catalytic metals (e.g., Pd, Pt, and Ni), which are most widely used for the hydrogenation of organic compounds, barely provide the selective reduction of nitro groups when other reducible groups are present in the same substrate, although adjustment of the solvent, catalyst support, and noble-metal particle size, as well as the addition of organic or inorganic modifiers, allow success to be attained in certain cases. During the last decade, it was found that functionalized anilines could be obtained with very high selectivity by hydrogenation of the corresponding nitroaromatic compounds over supported gold catalysts; these delivered lower reaction rates than those of palladium and platinum catalysts, but were much more chemoselective and did not require modifiers.[2,4–11] The superiority of gold catalysts in this respect was clearly confirmed by the fact that the introduction of a very small amount of palladium or platinum (100–2000 ppm) into gold nanoparticles resulted in a sharp drop in selectivity for the hydrogenation of a nitro group in the presence of C–Cl or C=C bonds.[7c,9d] It was also demonstrated that hydrogenation of nitroaromatics over gold catalysts was a structure-sensitive reaction that demanded a coordinatively unsaturated gold site for the activation/dissociation of $H_2$, and therefore, control of gold dispersion was essential to attain active catalysts.[2,4,7,11] Gold particles with diameters of less than 3 nm exhibit the highest catalytic activity expressed in terms of turnover frequency (TOF; as reaction rate per surface Au atom) or turnover number (TON; as reaction rate per Au concentration).[8,9,11] Viswanathan et al. also noted that the catalytic performance of supported gold strongly depended on the porous nature of the support because it might play an important role in stabilizing the efficient dispersion of gold nanoparticles or vice versa in facilitating metal particle agglomeration.[12]

To date, hydrogenation of aromatic nitro compounds was performed in either liquid-phase batch reactors[5–8] or gas-phase flow reactors[4,9,10] and, to the best of our knowledge, has never been examined under continuous liquid-phase flow conditions. Meanwhile, the last decade has witnessed rapid

[a] Dr. A. L. Nuzhdin, B. L. Moroz, Dr. G. A. Bukhtiyarova, Prof. S. I. Reshetnikov, P. A. Pyrjaev, P. V. Aleksandrov, Prof. V. I. Bukhtiyarov
Boreskov Institute of Catalysis 5
Prospect Akademika Lavrentieva 5
630090 Novosibirsk (Russia)
E-mail: gab@catalysis.ru

[b] B. L. Moroz, Prof. V. I. Bukhtiyarov
Novosibirsk State University 2
Pirogova Street, 630090 Novosibirsk (Russia)



© 2015 Wiley-VCH Verlag GmbH & Co. KGaA, Weinheim

growth in interest, both practical and academic, in performing the reactions for organic synthesis (including chemo- and enantioselective hydrogenation reactions) over solid catalysts in automated three-phase flow reactors.[13] Their use allows improved gas–liquid–solid interactions owing to large interfacial areas to reduce accumulation of side products through better control of process variables to limit contact of employees with toxic chemicals to which they may be exposed during cleaning of equipment. Herein, we describe the first examples of highly selective hydrogenation of several substituted nitrobenzenes, such as 2-, 3-, and 4-chloronitrobenzenes (2-, 3-, and 4-CNBs); 4-acetylnitrobenzene (4-ANB); and 3-vinylnitrobenzene (3-VNB), to give the corresponding anilines over 1.9% Au/γ-$Al_2O_3$ catalyst in a three-phase packed-bed reactor operating in up-flow mode at elevated temperatures and pressure.

## Results and Discussion

### Catalyst characterization

The Au/$Al_2O_3$ catalyst used herein was prepared through the adsorption of anionic gold(III) hydroxychloride complexes from an alkalized aqueous solution of H[$AuCl_4$] (the so-called deposition–precipitation (DP) method).[14] Treatment of alumina with a solution of H[$AuCl_4$] + NaOH at 70 °C, followed by washing and drying, produced a pale-yellow material that turned to dark violet upon calcination in air at 300 °C to indicate the formation of gold(0) nanoparticles. The as-prepared catalyst contained 1.9 wt% gold, as measured by X-ray fluorescence (XRF).

From the TEM data shown in Figure 1a, the Au/$Al_2O_3$ catalyst prepared by DP comprises mainly Au particles of 1.3–2.5 nm in diameter; there are also a few smaller ($d_i$ = 1.0–1.2 nm) and larger ($d_i$ = 2.6–3.1 nm) particles. The particle size distribution (shown in the inset in Figure 1a) is rather narrow with a maximum at approximately 2 nm with a standard deviation ($\sigma$) equal to 0.3.

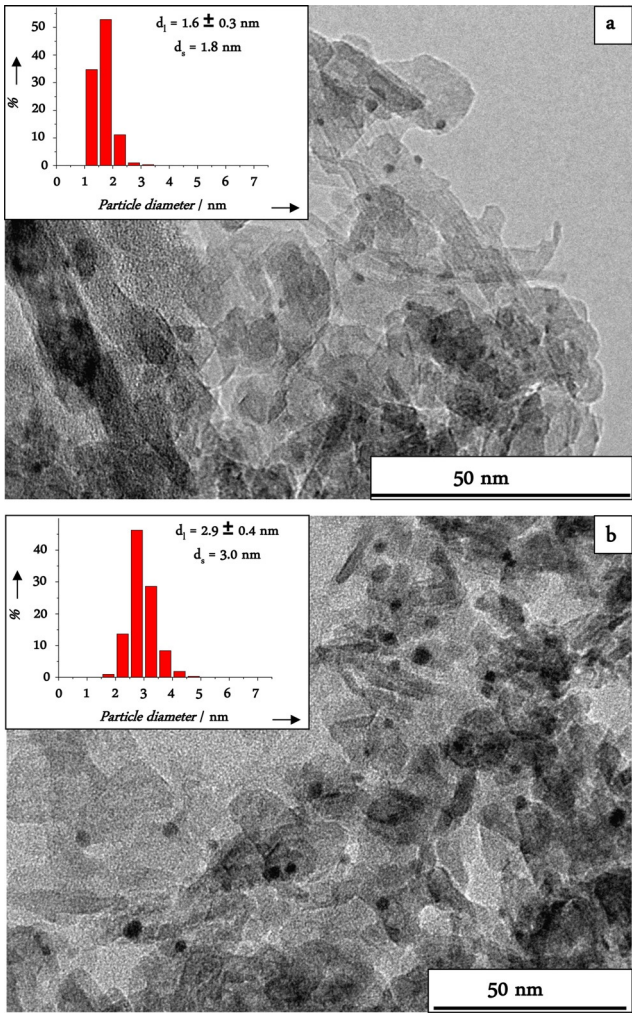


**Figure 1.** TEM images of the 1.9% Au/$Al_2O_3$ catalyst: a) as-prepared catalyst; b) the catalyst after testing for the hydrogenation of 3-VNB in toluene under continuous-flow conditions at 80 °C, $[3\text{-VNB}]_{inlet}$ = 0.05 M, $p(H_2)$ = 10 bar, and inlet $H_2$/3-VNB molar ratio = 107. The insets show gold particle size distributions in the samples ($d_i$ and $d_s$ stand for the mean linear and surface diameters, respectively).

### Hydrogenation of substituted nitrobenzenes

Hydrogenation of a nitro group in nitroaromatic compounds over supported gold catalysts may be limited by the external transfer of reactants to the catalyst surface and not by reaction kinetics. Studying the liquid-phase hydrogenation of benzene and α-methylstyrene over solid catalysts under continuous-flow conditions, which in many ways are similar to those examined herein, shows that external mass transfer is enhanced if the hydrogen flow rate at the reactor inlet is enlarged.[15] By taking this into account, a set of experiments was performed to examine the effect of hydrogen flow rate on the conversion of substituted nitrobenzene (3-VNB) over the Au/$Al_2O_3$ catalyst by increasing the $H_2$ flow rate from 8 to 60 mL min$^{-1}$ at a constant liquid velocity of 0.5 mL min$^{-1}$. Figure 2 illustrates the typical dependence of conversion and reaction selectivity on the flow rate of $H_2$ and reflects the existence of two regions. At low flow rates of $H_2$ from 8 to 30 mL min$^{-1}$, the conversion increases with increasing gas velocity. In this case, external mass transfer (most probably, dissolution of $H_2$ into the solution of

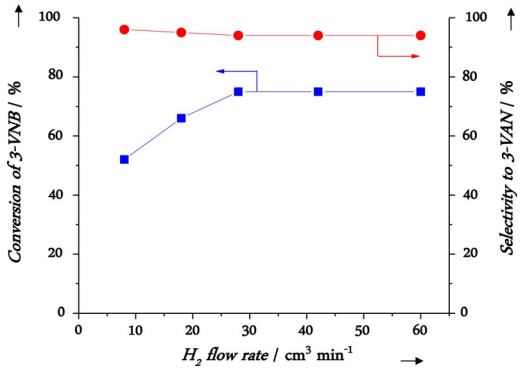


**Figure 2.** Effect of $H_2$ flow rate on the conversion of 3-VNB and selectivity to 3-vinylaniline (3-VAN) during hydrogenation of 3-VNB in toluene over the 1.9% Au/$Al_2O_3$ catalyst. Reaction conditions: a packed-bed flow reactor, $T$ = 70 °C, $[3\text{-VNB}]_{inlet}$ = 0.05 M, $p(H_2)$ = 10 bar, the mass of catalyst = 0.185 g, flow rate of the liquid phase = 0.5 mL min$^{-1}$, reaction time = 30 min.


© 2015 Wiley-VCH Verlag GmbH & Co. KGaA, Weinheim

21926506, 2015, 12, Downloaded from https://chemistry-europe.onlinelibrary.wiley.com/doi/10.1002/cplu.201500310 by Hokkaido University, Wiley Online Library on [06/10/2025]. See the Terms and Conditions (https://onlinelibrary.wiley.com/terms-and-conditions) on Wiley Online Library for rules of use; OA articles are governed by the applicable Creative Commons License

21926506, 2015, 12, Downloaded from https://chemistry-europe.onlinelibrary.wiley.com/doi/10.1002/cplu.201500310 by Hokkaido University, Wiley Online Library on [06/10/2025]. See the Terms and Conditions (https://onlinelibrary.wiley.com/terms-and-conditions) on Wiley Online Library for rules of use; OA articles are governed by the applicable Creative Commons License

nitroaromatic compound in toluene) seems to be the rate-determining step of the process. At higher flow rates of $H_2$ ($\geq$30 mL min$^{-1}$), the conversion of nitroaromatic compound and selectivity for hydrogenation of a nitro group are independent of the gas velocity, which indicates that, under these conditions, external mass-transfer limitations are absent. Subsequently, all catalytic tests were performed at a high hydrogen flow rate of 60 mL min$^{-1}$. As a result of special tests, we found that an enlargement of the catalyst grain sizes from 125–250 to 350–500 μm had no considerable effect on the conversion measured at a hydrogen flow rate of 60 mL min$^{-1}$, which implied negligible influence of internal mass transfer under the conditions used.

### *Hydrogenation of isomeric monochloronitrobenzenes*

Table 1 presents the results obtained with the 1.9%Au/$Al_2O_3$ catalyst for the liquid-phase hydrogenation of isomeric CNBs in a packed-bed flow reactor at 70–110 °C, with a $H_2$ flow rate of 60 mL min$^{-1}$ ($p(H_2)$ = 10 bar) and flow rate of a solution of CNB in toluene ([CNB]$_{inlet}$ = 0.05 M) equal to 0.5 mL min$^{-1}$ (inlet $H_2$/CNB molar ratio of 107). Under these conditions, CNB conversion was independent of the position of the Cl atom to the $NO_2$ group in the benzene ring and even at 70 °C reached about 97% with selectivities to 2-, 3-, or 4-CAN of 96.4, 95.5, or 97.3%, respectively (Table 1, entries 1, 4, and 8). In addition, 2-, 3-, or 4-CNSB and products of condensation with the corresponding chlorophenylhydroxylamine (CPHA), such as 1,2-bis(-chlorophenyl)diazene *N*-oxide, 1,2-bis(chlorophenyl)diazene, and 1,2-bis(chlorophenyl)hydrazine, were found in the reaction mixtures at the reactor outlet. All are key intermediates in the classical reaction mechanism for the hydrogenation of CNBs to CANs[2,16,17] (Scheme 1). No dechlorination products nor intermediate CPHA were detected by GC during the catalytic tests performed in this study, which indicated that, if they were produced in the reaction, it was only in negligible amounts.

**Table 1.** Liquid-phase hydrogenation of isomeric CNBs over the 1.9% Au/$Al_2O_3$ catalyst in a packed-bed flow reactor.[a]

| Entry | Substrate | $T$ [°C] | Conv. [%] | Selectivity [%] | | |
|---|---|---|---|---|---|---|
| | | | | CAN | CCNSB | Others |
| 1 | 2-Cl$C_6H_4NO_2$ | 70 | 96.7 | 96.4 | 3.6 | n.d. |
| 2 | 2-Cl$C_6H_4NO_2$ | 80 | 99.4 | 98.7 | 1.3 | n.d. |
| 3 | 2-Cl$C_6H_4NO_2$ | 90 | 100 | 100 | n.d. | n.d. |
| 4 | 3-Cl$C_6H_4NO_2$ | 70 | 97.3 | 95.5 | 3.8 | 0.7 |
| 5 | 3-Cl$C_6H_4NO_2$ | 80 | 99.2 | 97.8 | 1.5 | 0.7 |
| 6 | 3-Cl$C_6H_4NO_2$ | 90 | 100 | 99.0 | 0.6 | 0.4 |
| 7 | 3-Cl$C_6H_4NO_2$ | 110 | 100 | 100 | n.d. | n.d. |
| 8 | 4-Cl$C_6H_4NO_2$ | 70 | 96.7 | 97.3 | 1.4 | 1.3 |
| 9 | 4-Cl$C_6H_4NO_2$ | 80 | 100 | 98.6 | n.d. | 1.4 |
| 10 | 4-Cl$C_6H_4NO_2$[b] | 110 | 100 | 100 | n.d. | n.d. |

[a] Reaction conditions: [CNB]$_{inlet}$ = 0.05 M; solvent: toluene; $p(H_2)$ = 10 bar; mass of the catalyst: 0.185 g; flow rates of the liquid phase and $H_2$: 0.5 and 60 mL min$^{-1}$, respectively (inlet $H_2$/CNB molar ratio = 107); reaction time = 30–38 min. [b] Tested at $p(H_2)$ = 40 bar. CAN = chloroaniline, CNSB = chloronitrosobenzene, n.d. = not detected.

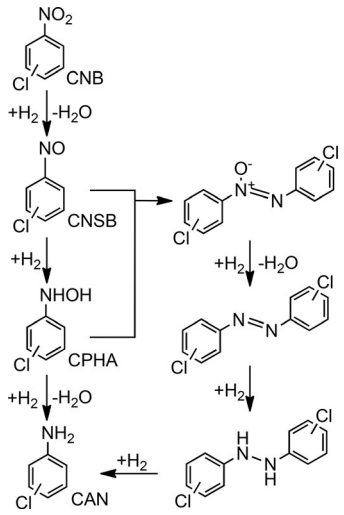


**Scheme 1.** Generally accepted reaction scheme for the hydrogenation of isomeric monochloronitrobenzenes into the corresponding CANs.

When the reaction temperature rises above 70 °C, selectivity for nitroso intermediates and its condensation products decreases, whereas selectivity to CANs increases accordingly. The 2-CAN product is formed from 2-CNB over the Au/$Al_2O_3$ catalyst in quantitative yield at a $H_2$ pressure of 10 bar and temperature as low as 90 °C, whereas obtaining the target product (3-CAN) through the hydrogenation of 3-CNB in 100% yield at the same pressure requires temperatures of not less than 110 °C (Table 1, entries 3 and 7). Finally, quantitative production of 4-CAN from 4-CNB requires not only to increasing the reaction temperature to 110 °C, but also increasing the hydrogen pressure to 40 bar (Table 1, entry 10). The difference observed in the product distributions of the hydrogenation of different isomeric CNBs under identical conditions may be related to the fact that the rate of interconversions of CNSB and its condensation products, as well as the rate of their transformation to CAN, depend on the mutual positions of the Cl atom and nitro group in the benzene ring.

### *Hydrogenation of 4-ANB*

Table 2 shows the results of liquid-phase 4-ANB hydrogenation over the Au/$Al_2O_3$ catalyst at 70–90 °C under continuous-flow conditions similar to those used for the hydrogenation of CNBs. The target product, 4-AAN, was formed with high selectivity ($\geq$94%) at any of the temperatures tested. In addition to 4-AAN, 4-VAN, 4-EAN, and a product of carbonyl–amine condensation of two 4-AAN molecules were detected in the reaction mixture at the outlet of reactor. It is likely that 4-VAN appears owing to hydrogenation of the carbonyl group in 4-AAN followed by dehydration of the intermediate 1-(4-aminophenyl)ethanol, whereas 4-EAN is formed by hydrogenation of 4-VAN (Scheme 2). The yield of the condensation product decreased as the reaction temperature increased (Table 2, entries 1 and 2), and at 90 °C it was not detected among the reaction products (Table 2, entry 3). On the contrary, the yield of the products of carbonyl group reduction (4-VAN and 4-EAN) increased


© 2015 Wiley-VCH Verlag GmbH & Co. KGaA, Weinheim

**Table 2.** Liquid-phase hydrogenation of 4-ANB over the 1.9% $Au/Al_2O_3$ catalyst in a packed-bed flow reactor.[a]

| Entry | $T$ [°C] | Conv. [%] | Selectivity [%] | | | |
|---|---|---|---|---|---|---|
| | | | 4-AAN | 4-VAN | 4-EAN | Others |
| 1 | 70 | 99.2 | 96.9 | 2.1 | n.d. | 1.0 |
| 2 | 80 | 100 | 97.0 | 2.7 | 0.1 | 0.2 |
| 3 | 90 | 100 | 93.6 | 5.2 | 1.2 | n.d. |

[a] Reaction conditions: $[4\text{-ANB}]_{inlet} = 0.05$ M; solvent: toluene; $p(H_2) = 10$ bar; mass of the catalyst: 0.185 g; flow rates of the liquid phase and $H_2$: 0.5 and 60 mL min$^{-1}$, respectively (inlet $H_2$/4-ANB molar ratio = 107); reaction time = 30–38 min. 4-AAN = 4-acetylaniline, 4-VAN = 4-vinylaniline, 4–EAN = 4-ethylaniline, n.d. = not detected.

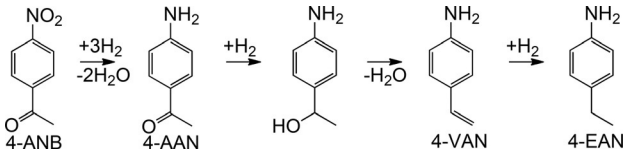


**Scheme 2.** Stepwise reaction pathway for the hydrogenation of 4-ANB.

with temperature, leading to a drop in selectivity to 4-AAN from 97% at 70–80 °C to 93.6% at 90 °C.

### *Hydrogenation of 3-VNB*

In Table 3, we report on the results obtained when the $Au/Al_2O_3$ catalyst was employed for the liquid-phase hydrogenation of 3-VNB under continuous-flow conditions. At temperatures as low as 60 °C (Table 3, entry 1), the conversion of 3-VNB reached approximately 57% with fairly good selectivity to the target product, 3-VAN, equal to 93.3%; the rest of the products were 3-VNSB and 3-EAN (Scheme 3). The TON value (at 60 °C), calculated as the amount of 3-VAN formed with time relative to the amount of catalyst (moles of Au), is 0.73 min$^{-1}$. Increasing the temperature to 80 °C led to an increase in the 3-VNB conversion up to approximately 98%. Simultaneously, the share of 3-VNSB, which was not further hydrogenated into 3-VAN, decreased, whereas the yield of 3-EAN, which was the product of the hydrogenation of the vinyl group in 3-VAN, increased almost equally (Table 3, entries 2 and 3). As a result, the selectivity to 3-VAN remained practically unchanged with reaction temperature.

**Table 3.** Liquid-phase hydrogenation of 3-VNB over the 1.9% $Au/Al_2O_3$ catalyst in a packed-bed flow reactor.[a]

| Entry | $T$ [°C] | Conv. [%] | Selectivity [%] | | |
|---|---|---|---|---|---|
| | | | 3-VAN | 3-VNSB | 3-EAN |
| 1 | 60 | 56.7 | 93.3 | 3.3 | 3.4 |
| 2 | 70 | 75.2 | 92.9 | 1.6 | 5.5 |
| 3 | 80 | 98.1 | 92.8 | 0.5 | 6.7 |

[a] Reaction conditions: $[3\text{-VNB}]_{inlet} = 0.05$ M; solvent: toluene; $p(H_2) = 10$ bar, mass of the catalyst: 0.185 g; flow rates of the liquid phase and $H_2$: 0.5 and 60 mL min$^{-1}$, respectively (inlet $H_2$/3-VNB molar ratio = 107); reaction time = 30–38 min. 3-VNSB = 3-vinylnitrosobenzene, 3-EAN = 3-ethylaniline.

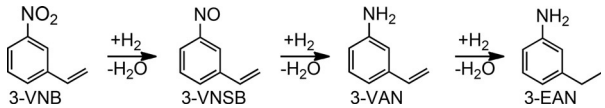


**Scheme 3.** Stepwise reaction pathway for the hydrogenation of 3-VNB.

The effect of residence time in the reactor on the 3-VNB conversion over the $Au/Al_2O_3$ catalyst was further studied at different reaction temperatures. The residence time ($\tau$) was fixed at a constant $H_2$ flow rate of 60 mL min$^{-1}$. Thus, during all experiments, a large excess of $H_2$ was maintained in the reaction media (inlet $H_2$/3-VNB molar ratio > 35) to avoid external mass-transfer limitations. Figure 3a displays the 3-VNB conversion measured 30–38 min after the start of the experiment versus $\tau$ for three different reaction temperatures. The experimental data are described by Equation (1):

$$X = 1 - e^{-k\tau} \quad (1)$$

in which $X$ is conversion of 3-VNB and $k$ is the rate constant. This indicates that the values of $k$ can be determined by fitting the experimental data to Equation (1). Plotting the graph of $\ln k$ versus $1/T$ results in a straight line, as shown in Figure 3b. The apparent activation energy, $E_a$, for 3-VNB hydrogenation over the $Au/Al_2O_3$ catalyst (within the temperature range from 60 to 80 °C) estimated from the slope of the Arrhenius plot is about 64 kJ mol$^{-1}$.

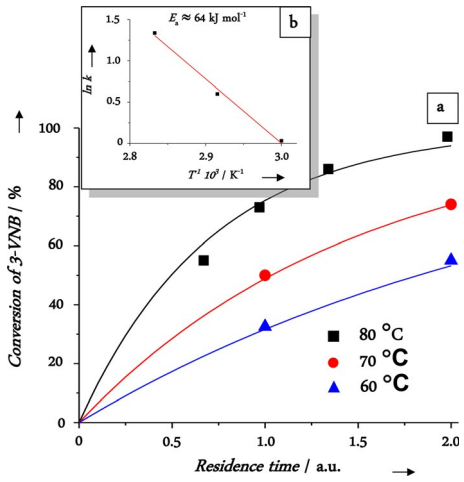


**Figure 3.** a) Conversion of 3-VNB over the 1.9% $Au/Al_2O_3$ catalyst as a function of residence time for different temperatures. The symbols represent the experimental data, whereas the lines represent the model fit to the experimental data. b) Arrhenius plot of the rate constant ($k$, s$^{-1}$) of 3-VNB hydrogenation. Reaction conditions: a packed-bed flow reactor; $[3\text{-VNB}]_{inlet} = 0.05$ M; solvent: toluene; $p(H_2) = 10$ bar; mass of the catalyst: 0.185 g; flow rates of the liquid phase and $H_2$: 0.5–1.5 and 60 mL min$^{-1}$, respectively; reaction time = 30–38 min.


© 2015 Wiley-VCH Verlag GmbH & Co. KGaA, Weinheim

21926506, 2015, 12, Downloaded from https://chemistry-europe.onlinelibrary.wiley.com/doi/10.1002/cplu.201500310 by Hokkaido University, Wiley Online Library on [06/10/2025]. See the Terms and Conditions (https://onlinelibrary.wiley.com/terms-and-conditions) on Wiley Online Library for rules of use; OA articles are governed by the applicable Creative Commons License

21926506, 2015, 12, Downloaded from https://chemistry-europe.onlinelibrary.wiley.com/doi/10.1002/cplu.201500310 by Hokkaido University, Wiley Online Library on [06/10/2025]. See the Terms and Conditions (https://onlinelibrary.wiley.com/terms-and-conditions) on Wiley Online Library for rules of use; OA articles are governed by the applicable Creative Commons License

### Catalyst deactivation and regeneration

The time-on stream performance of the $Au/Al_2O_3$ catalyst under the conditions of liquid-phase hydrogenation of substituted nitrobenzenes in a packed-bed flow reactor was studied at 80 °C and the hydrogen pressure of 10 bar for up to 2 h of continuous operation. During this period, liquid samples of the reaction flow were taken every 20 min at the reactor outlet and analyzed by GC. As a result, smooth deactivation of the catalyst with time on-stream was observed, regardless of the substrate used for hydrogenation. As an example, Figure 4a

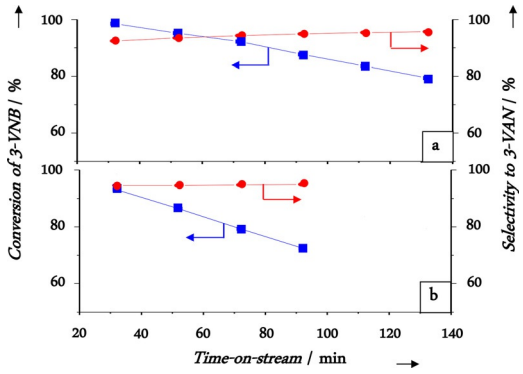


**Figure 4.** Time dependence of 3-VNB conversion and selectivity to 3-VAN during hydrogenation of 3-VNB over the 1.9% $Au/Al_2O_3$ catalyst taken a) as-prepared and b) after regeneration in a flow of air at 400 °C. Reaction conditions: a packed-bed flow reactor; $T = 80$ °C; $[3\text{-VNB}]_{inlet} = 0.05$ M; solvent: toluene; $p(H_2) = 10$ bar; mass of the catalyst: 0.185 g; flow rates of the liquid phase and $H_2$: 0.5 and 60 mL min$^{-1}$, respectively (inlet $H_2$/CNB molar ratio = 107); reaction time = 30–38 min.

demonstrates the time dependence of 3-VNB conversion and selectivity to 3-VAN over the $Au/Al_2O_3$ catalyst. A reduction in the conversion level from 98.5 to 79.5% occurred after 2 h on stream, whereas the selectivity remained practically unchanged during this period.

The loss of activity of supported gold catalysts was observed previously by conducting the hydrogenation of aromatic nitro compounds in both liquid-phase batch reactors[6, 7a, 11] and gas-phase flow reactors.[9c, e, 10b] This loss was explained by various reasons, including "irreversible" leaching of gold by the reaction medium;[18] aggregation of the smallest gold nanoparticles through both a dissolution–redeposition mechanism (Ostwald ripening of gold) and an on-surface sintering process aided by formed aromatic amines;[6, 11] and catalyst poisoning by strongly coordinated reaction intermediates, such as nitroso species.[16] In addition, coke formation seems to be a probable cause of catalyst deactivation because it has been observed during nitrobenzene hydrogenation over conventional palladium,[19] nickel,[20] and copper[21] catalysts supported on various carriers, such as $Al_2O_3$,[19a,b] MgO and hydrotalcite,[19b] activated carbon,[20] $SiO_2$,[21] and kieselghur.[21b] Carbonaceous deposits that might block the surface of catalytically active gold particles were found in the deactivated $Au/\gamma\text{-}Al_2O_3$ catalyst after it was used for gas-phase α-pinene isomerization at 190–210 °C.[22] Recently, Cárdenas-Lizana et al. established that deposition of carbonaceous species occluding the active sites was a cause of temporal deactivation of the $Au/Al_2O_3$ catalyst in the continuous gas-phase hydrogenation of 4-CNB at 150 °C and lower inlet $H_2$/4-CNB molar ratios ($H_2$/4-CNB ≤ 39).[9d]

To get an idea of the reasons for gold catalyst deactivation in the continuous liquid-phase hydrogenation of substituted nitrobenzenes, we conducted the following series of experiments. Approximately 2 h after starting the test with the $Au/Al_2O_3$ catalyst in 3-VNB hydrogenation at 80 °C and $p(H_2) = 10$ bar, a flow of pure toluene (1.5 mL min$^{-1}$) was fed into the reactor instead of a mixture of $H_2$ and the solution of 3-VNB in toluene, and the catalyst sample was washed at 80 °C for 10 min, then completely dumped out from the reactor and dried in vacuum (200 mbar) at 50 °C overnight. The spent catalyst was analyzed by XRF for gold content, as well as by temperature-programmed oxidation (TPO) and TEM techniques.

Figure 5 displays the results of a TPO study of the $Au/Al_2O_3$ catalyst taken before and after use in the liquid-phase 3-VNB hydrogenation under flow conditions. Each sample was studied in the equipment for thermogravimetric analysis (TGA) and DTA at the same time. The DTG curve of the fresh catalyst (Figure 5a) exhibits a broad peak with a maximum at approximately 95 °C, which is related, most likely, to removal of physically adsorbed water (the loss of the sample weight in the 25–250 °C range was 2.5%). Additionally, a weight loss of 1% was observed in the 250–500 °C range, probably owing to elimina-

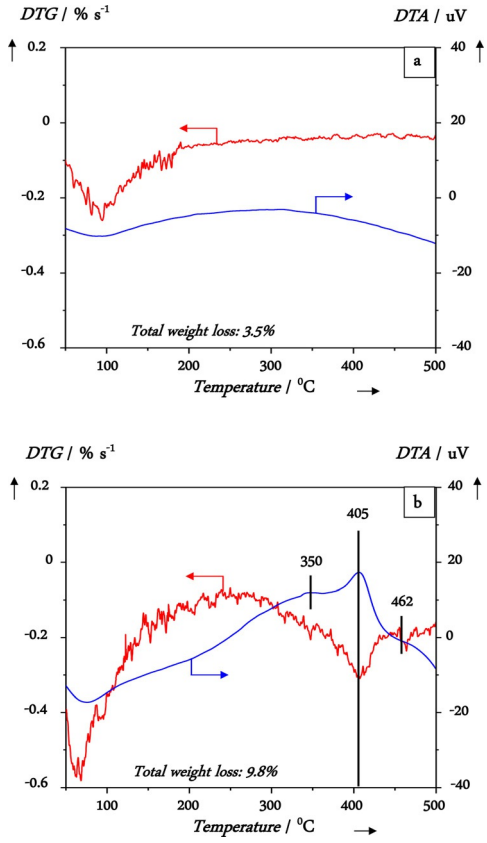


**Figure 5.** The differential thermogravimetric analysis (DTG)/differential thermal analysis (DTA) curves of a) as-prepared and b) spent $Au/Al_2O_3$ catalyst during TPO in a flow of air at a heating rate 10 °C min$^{-1}$.


© 2015 Wiley-VCH Verlag GmbH & Co. KGaA, Weinheim

tion of OH groups from the alumina surface. The DTA curve of the fresh sample contains an endothermic peak coinciding with weight loss owing to removal of adsorbed water and shows no signs of any exothermic reactions.

For the spent catalyst, the DTG curve measured under TPO conditions (Figure 5b) exhibits a two-stage weight loss over the 25–250 °C range with maxima at approximately 65 and 95 °C, which can be assigned to removal of the mixture of toluene and water adsorbed on the catalyst surface (the weight loss in this temperature range is 5.4%). In addition, upon heating to higher temperatures, the broad peak at 405 °C that corresponds to loss of 3.4% of the sample weight is observed. The DTA curve of the spent catalyst shows an endothermic peak in the temperature range from 50 to 100 °C related to removal of adsorbed toluene and water from the catalyst sample, and overlapping exothermic peaks at 350, 405, and 462 °C, which can be attributed to the combustion of carbonaceous species deposited onto the catalyst surface. The most distinct peak coincides well with the maximum weight loss at 405 °C. The positions of the exothermic peaks and ratio of their intensities closely resemble what was observed in the DTA profile generated in the TPO study of the $Au/Al_2O_3$ catalyst, which was preliminary deactivated during gas-phase α-pinene isomerization.[22] Assignment of these peaks was achieved based on the results of quantitative mass spectrometry analysis of the oxidation products evolved over different temperature ranges.[22] The formation of $CO_2$ as the main product during TPO of the spent $Au/Al_2O_3$ catalyst was observed starting from 350 °C up to approximately 500 °C with a maximum at 425–430 °C. Along with $CO_2$, traces of $H_2O$ appeared with a maximum yield at 409 °C. Taking this into account, the exothermic peaks at 350–360 and 405–410 °C may be attributed to oxidation of hydrogen-enriched carbonaceous species deposited onto the catalyst surface, whereas the exothermic peak at 460–470 °C can be assigned to combustion of surface amorphous carbonaceous deposits with a low hydrogen content. Cárdenas-Lizana et al.[9d] reported maximum heat release at 500 °C (i.e., at a temperature approximately 100 °C higher than that used in our study) during a TPO study of the $Au/Al_2O_3$ catalyst used in the continuous gas-phase hydrogenation of 4-CNB. This discrepancy may be explained by the fact that amorphous carbon lacking hydrogen ("coke") was mainly deposited on the catalyst surface instead of hydrogen-enriched carbonaceous species owing to the higher reaction temperature (150 °C) and lower inlet $H_2$/substrate molar ratios ($H_2$/4-CNB < 40) than those used in our study. Nevertheless, one can suggest that carbonaceous species are formed on the catalyst surface owing to adsorption of organic substrate, reaction intermediates, and products followed by their condensation and secondary transformations of the condensation products catalyzed, most probably, by Brønsted and Lewis acidic sites of alumina. Deposition of carbonaceous species appears to block the active sites of the $Au/Al_2O_3$ catalyst and be the reason for catalyst deactivation.

Regeneration of deactivated gold catalysts by burning-off carbon deposited on the catalyst surface has been applied for catalytic gas-phase oxidation,[23] isomerization,[22] and hydrogenation[9d] reactions. When studying the $Au/Al_2O_3$ catalyst deactivated during α-pinene isomerization,[22] it was found that oxidative treatment under a flow of air conducted up to 650 °C, which allows carbonaceous deposit accumulated on the catalyst surface to be burned off, has no considerable effect on the mean gold particle size and size distribution. This is in agreement with previous observations of the very high resistance of alumina-supported gold nanoparticles to sintering,[24] which is probably caused by epitaxial interactions between gold crystallites and the alumina surface.[24b]

The high sintering stability, which might be expected from the $Au/Al_2O_3$ catalyst, provides the possibility of restoring its activity in 3-VNB hydrogenation by burning-off surface carbonaceous species at temperatures of approximately 400 °C, which are sufficient for burning-off the main portion of these species, as observed in TPO experiments. For this purpose, the deactivated catalyst was heated in a fixed-bed Pyrex reactor with an air flow (500 $h^{-1}$) to 400 °C (ramping 4 °C $min^{-1}$) and then maintained at this temperature for 2 h. Figure 4b demonstrates that such a treatment restores 3-VNB conversion over the gold catalyst at 80 °C, $[3\text{-VNB}]_{inlet} = 0.05$ M, $H_2$/3-VNB molar ratio of approximately 100, and $\tau = 0.67$ s up to 93% (which is 94% of the initial $X$ value), although the selectivity to 3-VAN remains at the same level as that before regeneration.

Checking the gold content in the regenerated catalyst after use, we found that it was only 100 ppm less than the content in the as-prepared catalyst (1.87 wt% vs. 1.88 wt%), which was within the accuracy of XRF analysis. These results implied that irreversible gold leaching was negligible or absent, at least for the time that the catalytic run lasted. At the same time, a TEM study of the spent $Au/Al_2O_3$ catalyst (Figure 1b) demonstrated that the mean surface diameter ($d_s$) of the metal particles increased nearly twofold during 3-VNB hydrogenation at 80 °C ($d_s = 3.0$ nm vs. 1.8 nm in the as-prepared catalyst) owing to the appearance of numerous larger gold particles with sizes between 2.5 and 5 nm at the expense of the smallest metal particles of 1–2 nm in diameter. It seems unlikely that the growth of gold nanoparticles, which we have registered, was a result of their thermal sintering because the temperatures at which the catalytic reaction was performed (70–100 °C), were considerably lower than the calcination temperature during catalyst preparation (300 °C). One can assume that in the given case aggregation of the smallest gold nanoparticles proceeds through a dissolution–redeposition mechanism (the so-called Ostwald ripening of gold) and/or as an on-surface particle migration–coalescence process. Both can be aided by aromatic amine formed, which is present in the reaction stream in a high concentration and may interact with gold nanoparticles to promote their reversible dissolution in an organic solvent.[12] An increase in the $d_s$ value for gold particles registered after two successive catalytic runs means a decrease in the total surface of supported gold nanoparticles by a factor of 1.8 (assuming a simple model of gold nanospheres[25]) and the corresponding reduction in the observed activity of the catalyst if it is in direct proportion to the amount of surface gold atoms. Thus, the agglomeration of Au particles is probably another factor that causes the deactivation of the $Au/Al_2O_3$ catalyst


© 2015 Wiley-VCH Verlag GmbH & Co. KGaA, Weinheim

21926506, 2015, 12, Downloaded from https://chemistry-europe.onlinelibrary.wiley.com/doi/10.1002/cplu.201500310 by Hokkaido University, Wiley Online Library on [06/10/2025]. See the Terms and Conditions (https://onlinelibrary.wiley.com/terms-and-conditions) on Wiley Online Library for rules of use; OA articles are governed by the applicable Creative Commons License

during the liquid-phase hydrogenation of substituted nitrobenzenes under flow conditions. At the same time, because the reaction selectivity to 3-VAN was maintained with time on-stream and did not change as a result of catalyst recycling suggests a lack of influence of the formation of carbonaceous species and gold particle aggregation on the selectivity of hydrogenation of a nitro group in nitroaromatic compounds with other reducible functionalities.

## Conclusion

This study demonstrated the possibility of highly selective hydrogenation of a nitro group in a series of substituted nitrobenzenes with the general formula $XC_6H_4NO_2$, containing other reactive functionalities (X = Cl, CH=$CH_2$, or C(O)$CH_3$), in a continuous-flow three-phase reactor by using a nanodispersed Au/$Al_2O_3$ catalyst at lower temperatures than those usually used in batch reactors. The overall feed stream, which comprised of hydrogen and a solution of a substituted nitrobenzene in toluene, was passed through a packed catalyst bed at 60–110 °C and 10 bar in up-flow mode; hydrogen was fed to the reactor at a high flow rate ($\geq$30 mL $min^{-1}$) to avoid external mass-transfer limitations. One important result found was that hydrogenation of isomeric CNBs over the Au/$Al_2O_3$ catalyst under the above conditions gave the targeted CANs with almost 100% yield (100% selectivity at nearly 100% conversion); no formation of dechlorination products was detected. Increasing the reaction temperature and hydrogen pressure promoted the complete hydrogenation of nitroso intermediates, and thus, avoided the formation of products of their condensation with CPHA. Hydrogenation of 4-ANB and 3-VNB led to the formation of 3-VAN and 4-AAN with selectivities of up to 93 and 97% at substrate conversions as high as 98 and 100%, respectively. In these cases, increasing the reaction temperature favored C=C and C=O hydrogenation and resulted in minor detrimental changes in selectivity to the target anilines. A smooth deactivation of the catalyst with time on-stream was observed, regardless of which substituted nitrobenzene was used in hydrogenation. TEM and TPO studies of the Au/$Al_2O_3$ catalyst after testing for 3-VNB hydrogenation at 80 °C showed a nearly twofold increase in the mean surface diameter of gold particles during the reaction and the appearance of carbonaceous deposit on the catalyst surface which might block catalytically active sites. Oxidative regeneration of the spent catalyst sample in a flow of air at 400 °C restored its activity almost to the starting level with retention of high selectivity to 3-VAN. Taking this into consideration, we can suggest that the formation of carbonaceous deposit, which was probably promoted by Brønsted and Lewis acidic sites of the alumina support, was the main reason for catalyst deactivation. Thus, research efforts should be directed toward preventing this by modification of the support surface and optimization of reaction parameters. Aggregation of gold nanoparticles during the reaction seems to be less important, although understanding the reasons for and preventing this phenomenon are also an essential goal.

## Experimental Section

### General

An aqueous solution of H[$AuCl_4$]·(49.47 wt% Au) from Aurat (Russia) was used as the source of gold to prepare the gold catalyst. 3-VNB and 4-ANB (both 97% pure) and 2- and 4-CNBs (both 99% pure) from Acros Organics, as well as 3-CNB (98% pure) from Aldrich, were used as reagents for catalyst testing without further purification. Toluene of 99.5% purity from ECOS closed joint-stock company (Russia) and *n*-decane (>99% pure) from Acros Organics were employed as the solvent and internal GC standard, respectively, for catalytic experiments.

### Catalyst preparation

As the catalyst support, we used γ-$Al_2O_3$ (BET specific surface area: 215 $m^2 g^{-1}$, total pore volume: 0.61 $cm^3 g^{-1}$, mean pore diameter: 9.6 nm) prepared by extrusion of a paste consisting of aluminum oxide of Puralox TH 100/150 grade and aluminum hydroxide of Pural SB grade (both produced by Sasolchemie GmbH, Germany) mixed in a ratio of 30:70 by weight and added with an aqueous solution of nitric acid as a peptizing agent. The cylindrical $Al_2O_3$ granules of 1.5 mm in diameter thus obtained were dried at 110 °C overnight and calcined in a flow of air at 550 °C for 4 h. Then they were crushed and sieved to obtain support grains of 250–500 μm in diameter. The support was dried at 110 °C in a drying oven for 8 h immediately before gold deposition. The method for preparing the Au/$Al_2O_3$ catalyst was similar to those described previously:[14] A weighed amount of alumina support was shaken with an aqueous solution of H[$AuCl_4$] + NaOH (2.5 g Au per L) at 70 °C and pH 7 for 1 h in a constant-volume glass reactor, washed several times with large portions of warm distilled water (200 mL $g^{-1}$), dried in vacuo at room temperature for 14 h, and calcined in air at 300 °C for 4 h.

### Catalyst characterization

The Au contents of fresh and spent catalyst samples were measured in vacuo by using the XRF technique on an ARL instrument equipped with a Rh anode (X-ray tube voltage: 50 kV, tube current: 40 mA, exposure time: 10 s). TEM studies were performed by using a JEM-2010 (JEOL, Japan) electron microscope with a lattice resolution of 0.14 nm and a 200 kV accelerating voltage. The number-weighted ($d_l$) and surface-weighted ($d_s$) mean diameters of gold particles for each catalyst sample were determined by counting over 350 particles in TEM images taken with medium magnification and calculated according to Equations (2) and (3) derived by assuming a simple model of metal nanospheres:[25]

$$d_l = \Sigma d_i / N \quad (2)$$

$$d_s = \Sigma (d_i)^3 / (d_i)^2 \quad (3)$$

in which $d_i$ is the measured diameter of a metal particle and $N$ is the total number of particles. A TPO study of the fresh and used catalysts was performed on a NETZSCH STA 449C Jupiter instrument. The sample (30 mg) in a corundum crucible was placed on a thermobalance was heated from 25 to 500 °C (ramping 10 °C $min^{-1}$) under a slow of air. As a reference sample, calcined silica was used.


© 2015 Wiley-VCH Verlag GmbH & Co. KGaA, Weinheim

21926506, 2015, 12, Downloaded from https://chemistry-europe.onlinelibrary.wiley.com/doi/10.1002/cplu.201500310 by Hokkaido University, Wiley Online Library on [06/10/2025]. See the Terms and Conditions (https://onlinelibrary.wiley.com/terms-and-conditions) on Wiley Online Library for rules of use; OA articles are governed by the applicable Creative Commons License

21926506, 2015, 12, Downloaded from https://chemistry-europe.onlinelibrary.wiley.com/doi/10.1002/cplu.201500310 by Hokkaido University, Wiley Online Library on [06/10/2025]. See the Terms and Conditions (https://onlinelibrary.wiley.com/terms-and-conditions) on Wiley Online Library for rules of use; OA articles are governed by the applicable Creative Commons License

### General procedure for the hydrogenation of substituted nitrobenzenes

Hydrogenation of substituted nitrobenzenes in organic medium (toluene) to the corresponding anilines was performed under continuous-flow conditions in a H-Cube Pro setup (Thalesnano, Hungary) equipped with an electrolytic cell for the generation of high-purity hydrogen by in situ water electrolysis, a conventional HPLC pump for delivering a liquid reactant, and a touch-screen module for automatic control of operational parameters (reaction temperature and pressure, flow rates of hydrogen and liquid substrate, etc.). A more detailed description of the H-Cube Pro setup has been published elsewhere.[13a,26] A stainless-steel packed-bed CatCart30 reactor (catalyst cartridge) of 30 mm in length and 4.0 mm in inner diameter (volume 0.38 $cm^3$) preloaded with a catalyst sample (0.185 g) was installed in a stainless-steel heater controlled by using the Peltier unit. Immediately prior to the catalytic run, pure toluene solvent was passed through the connecting lines and reactor at a flow rate of 0.5 mL $min^{-1}$ to remove air. After air was removed from the connecting line and reactor, the desired reaction parameters were selected and the mixture of hydrogen and solvent was fed to the reactor in up-flow mode with a rate of 60 and 0.5 mL $min^{-1}$, respectively, until the required temperature and pressure were reached. The inlet was then switched to the flask filled with a 0.05 M solution of an organic substrate in toluene containing *n*-decane as an internal standard. This moment was chosen as the starting point of the reaction. The liquid flow was mixed with hydrogen in a gas/liquid mixer and fed to the reactor at a rate of 0.5 mL $min^{-1}$. The catalytic tests were usually performed at 60–110 °C, with a hydrogen pressure and flow rate of 10 bar and 60 mL $min^{-1}$, respectively. Typically, collection of the first sample of liquid product for analysis started 30 min after feeding of the substrate and continued for 4 min; immediately thereafter, the second sample was taken for another 4 min. The conversion of substituted nitrobenzene, selectivity to the determined product, and yield were calculated based on mean analysis results for these samples. Because the catalytic activity was reduced gradually under the experimental conditions, a fresh catalyst sample was taken for each catalytic run. The inlet and outlet concentrations of substrate and products were analyzed by means of a gas chromatograph (Agilent 6890N) equipped with a flame-ionization detector (FID) and a capillary HP 5-MS column (60 m × 0.32 mm × 0.25 μm). Reaction products were identified by GC/MS by using an Agilent 7000B Triple Quad System equipped with an HP 5-MS column. The conversion of substituted nitrobenzene, *X* (%), and the selectivity, *S* (%), to the determined product were calculated by using Equations (4) and (5), respectively:

$$X(\%) = \{([\text{substrate}]_{in} - [\text{substrate}]_{out})/[\text{substrate}]_{in}\} \times 100 \quad (4)$$

$$S(\%) = \{([\text{product}]_{out}/([\text{product}]_{in}) - [\text{product}]_{out}\} \times 100 \quad (5)$$

During all tests, the carbon balance between the inlet and outlet streams was within (95 ± 2) %.

## Acknowledgements

*We thank Dr. E. Yu. Gerasimov, Dr. M. V. Shashkov, I. L. Kraevskaya, and G. S. Litvak for their help in performing this study. Financial support of the study by the Russian Foundation for Basic Research (grant no. 13-03-12178) and the Grant of President of Russian Federation for government support of Leading Scientific Schools (grant SS-5340.2014.3) is gratefully acknowledged.*

**Keywords:** gold · hydrogenation · nitrobenzenes · supported catalysts · three-phase flow reactor

[1] R. S. Downing, P. J. Kunkeler, H. Van Bekkum, *Catal. Today* **1997**, *37*, 121–136.
[2] a) H.-U. Blaser, *Science* **2006**, *313*, 312–313; b) H.-U- Blaser, H. Steiner, M. Studer, *ChemCatChem* **2009**, *1*, 210–221.
[3] a) P. N. Rylander, *Hydrogenation Methods*, Academic Press, London, **1985**; b) R. L. Augustine, *Heterogeneous Catalysis for the Synthetic Chemist*, Marcel Dekker, New York, **1995**; c) S. Nishimura, *Handbook of Heterogenous Catalytic Hydrogenation for Organic Synthesis*, Wiley, New York, **2001**; d) H.-U. Blaser, A. Schnyder, H. Steiner, F. Rossler, P. Baumeister in *Handbook of Heterogeneous Catalysis, 2nd ed.*,(Eds.: G. Ertl, H. Knozinger, F. Schuth, J. Weitkamp), Wiley-VCH, Weinheim, **2008**, p. 3284; e) A. Kulkarni, B. Torok, *Curr. Org. Synth.* **2011**, *8*, 187–207.
[4] F. Cárdenas-Lizana, M. A. Keane, *J. Mater. Sci.* **2013**, *48*, 543–564.
[5] Y. Chen, J. Qiu, X. Wang, J. Xiu, *J. Catal.* **2006**, *242*, 227–230.
[6] D. He, H. Shi, Y. Wu, B.-Q. Xu, *Green Chem.* **2007**, *9*, 849–851.
[7] a) A. Corma, P. Serna, *Science* **2006**, *313*, 332–334; b) M. Boronat, P. Concepcion, A. Corma, S. Gonzalez, F. Illas, P. Serna, *J. Am. Chem. Soc.* **2007**, *129*, 16230–16237; c) P. Serna, P. Concepcion, A. Corma, *J. Catal.* **2009**, *265*, 19–25; <lit d>P. Serna, M. Boronat, A. Corma, *Top. Catal.* **2011**, *54*, 439–446.
[8] K. Shimizu, Y. Miyamoto, T. Kawasaki, T. Tanji, Y. Tai, A. Satsuma, *J. Phys. Chem. C* **2009**, *113*, 17803–17810.
[9] a) F. Cárdenas-Lizana, S. Gómez-Quero, M. A. Keane, *Catal. Commun.* **2008**, *9*, 475–481; b) F. Cárdenas-Lizana, S. Gómez-Quero, M. A. Keane, *ChemSusChem* **2008**, *1*, 215–221; c) F. Cárdenas-Lizana, S. Gómez-Quero, N. Perret, M. A. Keane, *Gold Bull.* **2009**, *42*, 124–132; d) F. Cárdenas-Lizana, S. Gómez-Quero, A. Hugon, L. Dellanoy, C. Louis, M. A. Keane, *J. Catal.* **2009**, *262*, 235–243; e) F. Cárdenas-Lizana, D. Lamey, M. Li, M. A. Keane, L. Kiwi-Minsker, *Chem. Eng. J.* **2014**, *255*, 695–704.
[10] a) X. D. Wang, N. Perret, M. A. Keane, *Chem. Eng. J.* **2012**, *210*, 103–113; b) N. Perret, X. D. Wang, T. Onfroy, C. Calers, M. A. Keane, *J. Catal.* **2014**, *309*, 333–342.
[11] U. Hartfelder, C. Kartusch, M. Makosch, M. Rovezzi, J. Sa, J. A. van Bokhoven, *Catal. Sci. Technol.* **2013**, *3*, 454–461.
[12] S. Viswanathan, B. Narayanan, Z. Yaakob, P. Periyat, S. Padikkaparambii, *J. Porous Mater.* **2014**, *21*, 251–262.
[13] a) G. Szollosi, S. Cserényi, F. Fülöp, M. Bartók, *J. Catal.* **2008**, *260*, 245–253; b) V. Hessel, *Chem. Eng. Technol.* **2009**, *32*, 1655–1681; c) S. Cserényi, G. Szöllősi, K. Szőri, F. Fülöp, M. Bartók, *Catal. Commun.* **2010**, *12*, 14–19; d) M. Irfan, T. N. Glasnov, C. O. Kappe, *ChemSusChem* **2011**, *4*, 300–316; e) G. Szőllősi, Z. Makra, F. Fülöp, M. Bartók, *Catal. Lett.* **2011**, *141*, 1616–1620; f) I. R. Baxendale, L. Brocken, C. J. Mallia, *Green Process Synth.* **2013**, *2*, 211–230; g) I. R. Baxendale, *J. Chem. Technol. Biotechnol.* **2013**, *88*, 519–552; h) C. Wiles, P. Watts, *Green Chem.* **2014**, *16*, 55–62.
[14] a) S. Tsubota, M. Haruta, T. Kobayashi, A. Ueda, Y. Nakahara, *Stud. Surf. Sci. Catal.* **1991**, *63*, 695–704; b) B. L. Moroz, P. A. Pyrjaev, V. I. Zaikovskii, V. I. Bukhtiyarov, *Catal. Today* **2009**, *144*, 292–305.
[15] a) K. C. Metaxas, N. G. Papayannakos, *Ind. Eng. Chem. Res.* **2006**, *45*, 7110–7119; b) S. Haase, M. Weiss, R. Langsch, T. Bauer, R. Lange, *Chem. Eng. Sci.* **2013**, *94*, 224–236; c) R. Langsch, J. Zalucky, T. S. Haase, R. Lange, *Chem. Eng. Process.* **2014**, *75*, 8–18.
[16] G. Richner, J. A. van Bokhoven, Y.-M. Neuhold, M. Makosch, K. Hungerbuchler, *Phys. Chem. Chem. Phys.* **2011**, *13*, 12463–12471.
[17] A. Corma, P. Concepcion, P. Serna, *Angew. Chem. Int. Ed.* **2007**, *46*, 7266–7269; *Angew. Chem.* **2007**, *119*, 7404–7407.
[18] C. Kartusch, F. Krumeich, O. Safonova, U. Hartfelder, M. Makosch, J. Sa, J. A. van Bokhoven, *ACS Catal.* **2012**, *2*, 1394–1403.
[19] a) E. Klemm, B. Amon, H. Redlingshofer, E. Dieterich, G. Emig, *Chem. Eng. Sci.* **2001**, *56*, 1347–1353; b) P. Sangeetha, K. Shanthi, K. S. R. Rao, B. Viswanathan, P. Selvam, *Appl. Catal. A* **2009**, *353*, 160–165.
[20] A. Nieto-Márquez, S. Gil, A. Romero, J. L. Valverde, S. Gómez-Quero, M. A. Keane, *Appl. Catal. A* **2009**, *363*, 188–198.


© 2015 Wiley-VCH Verlag GmbH & Co. KGaA, Weinheim

[21] a) L. Petrov, K. Kumbilieva, N. Kirkov, *Appl. Catal.* **1990**, *59*, 31 – 43; b) S. Diao, W. Qian, G. Luo, F. Wei, Y. Wang, *Appl. Catal.* **2005**, *286*, 30 – 35.
[22] I. L. Simakova, Yu. S. Solkina, B. L. Moroz, O. A. Simakova, S. I. Reshetnikov, I. P. Prosvirin, V. I. Bukhtiyarov, V. N. Parmon, D. Yu. Murzin, *Appl. Catal. A* **2010**, *385*, 136 – 143.
[23] P. Konova, A. Naydenov, T. Tabakova, D. Mehandjiev, *Catal. Commun.* **2004**, *5*, 537 – 542.
[24] a) S. Ivanova, C. Petit, V. Pitchon, *Gold Bull.* **2006**, *39*, 3 – 8; b) B. L. Moroz, D. A. Zyuzin, V. I. Zaikovskii, A. N. Shmakov, P. A. Pyrjaev, E. M. Moroz, V. I. Bukhtiyarov, *Extended Abstr. of the 9th European Conference on Catalysis "Catalysis for a Sustainable World"*, EuropaCat IX, Salamanca, Spain, **2009**, p. P10 – 108.
[25] J. R. Anderson, *Structure of Metallic Catalysts*, Academic Press, London, **1975**.
[26] a) R. V. Jones, L. Godorhazy, N. Varga, D. Szalay, L. Urge, F. Darvas, *J. Comb. Chem.* **2006**, *8*, 110 – 116; b) J. Chen, K. Przyuski, R. Roemmele, R. P. Bakale, *Org. Process Res. Dev.* **2014**, *18*, 1427 – 1433.

Manuscript received: July 9, 2015
Accepted Article published: August 5, 2015
Final Article published: August 28, 2015


© 2015 Wiley-VCH Verlag GmbH & Co. KGaA, Weinheim

21926506, 2015, 12, Downloaded from https://chemistry-europe.onlinelibrary.wiley.com/doi/10.1002/cplu.201500310 by Hokkaido University, Wiley Online Library on [06/10/2025]. See the Terms and Conditions (https://onlinelibrary.wiley.com/terms-and-conditions) on Wiley Online Library for rules of use; OA articles are governed by the applicable Creative Commons License